TOXICOLOGICAL SCIENCES **94(1)**, 206–216 (2006)
doi:10.1093/toxsci/kfl078
Advance Access publication August 17, 2006

Hepatic Gene Expression Profiling and Lipid Homeostasis in Mice Exposed to Steatogenic Drug, Tetracycline

Hu-Quan Yin,* Mingoo Kim,† Ju-Han Kim,†,‡ Gu Kong,§ Mi-Ock Lee,* Kyung-Sun Kang,¶ Byung-IL Yoon,‖ Hyung-Lae Kim,||| and Byung-Hoon Lee*,[1]

*College of Pharmacy and Research Institute of Pharmaceutical Sciences, Seoul National University, Seoul 151-742, Republic of Korea; †Seoul National University Biomedical Informatics and ‡Human Genome Research Institute, College of Medicine, Seoul National University, Seoul 110-799, Republic of Korea; §College of Medicine, Hanyang University, Seoul133-791, Republic of Korea; ¶College of Veterinary Medicine, Seoul National University, Seoul 151-742, Republic of Korea; ‖College of Veterinary Medicine, Kangwon National University, Chuncheon 200-791, Republic of Korea; and |||College of Medicine, Ewha Womans University, Seoul 158-710, Republic of Korea

Received May 30, 2006; accepted August 3, 2006

Tetracycline is one of a group of drugs known to induce microvesicular steatosis. In the present study, we investigated the effects of tetracycline on gene expression in mouse liver, using Applied Biosystems Mouse Genome Survey Microarrays. A single oral dose of 0.1 or 1 g/kg tetracycline was administered to male ICR mice, and liver samples were obtained after 6, 24, or 72 h. Histopathological evaluation showed microvesicular steatosis in the high-dose group at 24 h. In total, 96 genes were identified as tetracycline responsive. Their level of expression differed significantly from controls (two-way analysis of variance; $p < 0.05$), after adjustment by the Benjamini-Hochberg multiple testing correction, and displayed a twofold or greater induction or repression. The largest groups of gene products affected by tetracycline exposure were those involved in signal transduction, nucleic acid metabolism, developmental processes, and protein metabolism. The expression of genes known to be involved in lipid metabolism was examined, using two-sample Student's *t*-test for each treatment group versus a corresponding control group. The overall net effects on expression of lipid metabolism genes indicated an increase in cholesterol and triglyceride biosynthesis and a decrease in β-oxidation of fatty acids. Our data support a proposed mechanism for tetracycline-induced steatogenic hepatotoxicity that involves these processes. Moreover, we demonstrated global changes in hepatic gene expression following tetracycline exposure; many of these genes have the potential to be used as biomarkers of exposure to steatogenic hepatotoxic agents.

Key Words: **tetracycline; microvesicular steatosis; toxicogenomics; lipid metabolism; microarray.**

The observation of toxicity in animals or of adverse reactions in humans are compelling reasons for terminating a drug's development, as well as for postmarketing withdrawal. Among the toxic side effects seen in animal testing and in clinical trials, hepatotoxicity is the principal cause of termination for safety reasons (Ballett, 1997; Lumley and Walder, 1987a,b). Animals that are frequently used in toxicity tests are not fully predictive of the response in humans due to species variation in physiology, anatomy, and metabolism. The number of animals, the dose of the drug, and the duration of the experiment are also critical limiting factors. Therefore, practical needs exist for establishing new predictive toxicology methods. Toxicogenomic or *in silico* technologies are currently popular as fast and cost-efficient alternatives or supplements to bioassays for the identification of toxic effects at an early stage of drug development (Helma, 2005; Storck *et al.*, 2002; Suter *et al.*, 2004).

Tetracyclines are a well-known family of antibiotics that are active against a wide range of gram-positive and gram-negative bacteria. In addition, anti-inflammatory properties of tetracycline, which are independent of its antibacterial activity, have been described (Gabler *et al.*, 1992). Tetracycline induces microvesicular steatosis in the liver, which is severe and even fatal in some vulnerable patients (Bhagavan *et al.*, 1982; Westphal *et al.*, 1994). Although formerly considered a benign and fully reversible condition, hepatic fatty infiltration is an important pathogenic factor in the development of many drug-induced liver diseases. Tetracyclines downregulate the expression of peroxisome proliferator activated receptors, which are widely used in the well-established Tet-off systems for studying inducible gene expression (Tachibana *et al.*, 2005; Wu *et al.*, 1996). Freneaux *et al.* (1988) demonstrated the inhibition of mitochondrial β-oxidation of fatty acids by tetracycline in mice. Similarly, Amacher and Martin (1997) showed that the canine hepatocyte is susceptible to tetracycline-induced steatosis, when triglyceride (TG) accumulation was concomitant with the inhibition of mitochondrial lipid metabolism.

Large-scale gene expression analysis provides a logical approach to studying the detailed mechanisms of chemical-induced organ toxicity as well as to identifying potential biomarkers of toxicity. To identify global gene expression

[1] To whom correspondence should be addressed at College of Pharmacy, Seoul National University, San 56-1, Sillim-dong, Gwanak-gu, Seoul 151-742, Republic of Korea. Fax: +82-2-874-7843. E-mail: lee@snu.ac.kr.

changes that are associated with hepatotoxicity and to better understand the molecular mechanisms underlying tetracycline-induced steatosis, we investigated the effects of tetracycline on gene expression in mouse liver across multiple doses and time points, with special emphasis on genes associated with lipid metabolism.

MATERIALS AND METHODS

Animal treatments. Specific pathogen-free male ICR mice (20–25 g) were obtained from Jung-Ang Laboratory Animal Co. (Seoul, Korea) and allowed free access to standard chow and tap water. They were kept in temperature-controlled and filter-sterilized animal quarters under a 12-h light:12-h dark cycle. The use of animals was in compliance with the guidelines established by the Animal Care Committee of this institute. A total of 27 mice (nine per group) were given a single oral dose of 0.1 g/kg (low-dose group, L), 1 g/kg (high-dose group, H), or distilled water (control group, C), and three from each group were subsequently killed at 6 (C6, L6, and H6), 24 (C24, L24, and H24), or 72 h (C72, L72, and H72). The dose was selected by preliminary experiments that induce mild hepatic steatosis at 24 h. A cross section of the left lateral lobe of the liver was collected in 10% neutral-buffered formalin for histopathology. The remaining liver tissue was collected in RNase-free tubes and snap frozen in liquid nitrogen. Frozen tissues were stored at − 70°C until processed for RNA extraction.

Clinical chemistry and histological analysis. Serum samples were prepared from blood withdrawn by heart puncture, using standard methods. Serum levels of alanine aminotransferase (ALT), alkaline phosphatase, blood urea nitrogen, creatinine, total bilirubin, TG, and albumin were monitored by standard clinical chemistry assays on an Automated Chemistry Analyzer (Prestige 24I; Tokyo Boeki Medical System, Tokyo, Japan). Liver tissues collected in formalin were dehydrated, embedded in paraffin, sectioned at 4 μm, and stained with hematoxylin and eosin. Histopathologic examinations of the liver sections were conducted by a pathologist and were peer reviewed.

RNA isolation. Total RNA was extracted using an Easy-Blue total RNA extraction kit (Intron Biotech, Sungnam, Korea), purified using Qiagen RNeasy Mini Kits (Qiagen, Basel, Switzerland), and examined for integrity using an Agilent 2100 Bioanalyzer (Ambion, Austin, TX).

Microarray analysis of differential gene expression. Applied Biosystems (Foster City, CA) Mouse Genome Survey Microarrays were used to analyze differential gene expression profiles. These arrays contain 32,996 probes that cover 44,498 individual transcripts and target a complete, annotated, and fully curated set of 32,381 mouse genes from the public and Celera databases. RNA extracted from the livers of three mice was analyzed for each time point (6, 24, and 72 h) and for each treatment. Digoxigenin-UTP–labeled cRNA was generated and linearly amplified from 2 μg of total RNA using an Applied Biosystems Chemiluminescent RT-IVT Labeling Kit v2.0. Array hybridization, chemiluminescence detection, image acquisition, and analysis were performed using an Applied Biosystems Chemiluminescence Detection Kit and an Applied Biosystems 1700 Chemiluminescent Microarray Analyzer, following the manufacturer's protocol. Briefly, each microarray was first prehybridized at 55°C for 1 h in hybridization buffer with blocking reagent. Ten micrograms of labeled cRNA targets were incubated with fragmentation buffer at 60°C for 30 min and hybridized to each microarray in a 0.5-ml volume at 55°C for 16 h. Images were autogridded, and spots were spatially normalized. Chemiluminescent signals were quantified, corrected for background, and the final images and feature data were processed using the Applied Biosystems 1700 Chemiluminescent Microarray Analyzer v1.1.

Data analysis. The quality of hybridization and overall chip performance were monitored by visual inspection of both internal quality control checks and the raw scanned data. Assay-normalized signals with quality flags lower than 100 were used for the analysis. Filtered values were imputed by a k-nearest neighbors imputation algorithm (Troyanskaya *et al.*, 2001), transformed by the variance-stabilizing normalization method (Huber *et al.*, 2002), and normalized by quantile normalization across the arrays (Bolstad *et al.*, 2003).

The overall flow of data analysis is illustrated in Figure 1. Two-way analysis of variance (ANOVA) was applied to determine both time and dose effects and differentially expressed sets of genes. Statistical significances were adjusted by Benjamini-Hochberg multiple testing correction. Hierarchical clustering was performed with the Cluster/TreeView analytic package (Eisen, Stanford University, CA). Biological pathway and ontology-based analysis were performed by using Panther database (http://www.pantherdb.org) and ArrayX Path (http://www.snubi.org/software/ArrayXPath/). *Post hoc* two-sample Student's *t*-tests were performed. Default parameters from *R* statistical package

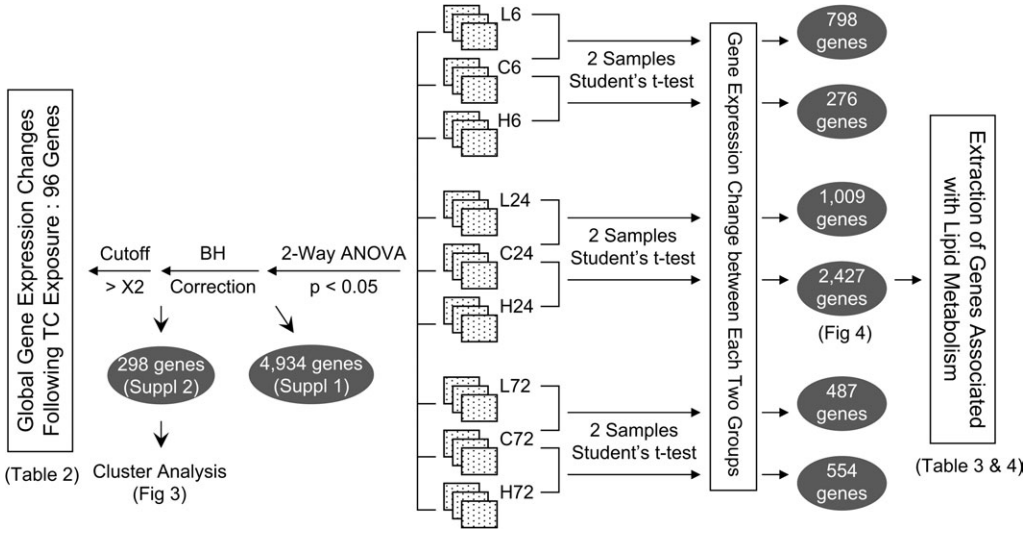

FIG. 1. Flow chart for data analysis. The microarray data were analyzed by two-way ANOVA for identifying global gene expression changes and by two-sample Student's *t*-test for investigating genes associated with lipid metabolism at specific treatment conditions.

TABLE 1
Gene-Specific Primers Used in qRT-PCR

Gene	NCBI RefSeq	Forward primer (5′–3′)	Reverse primer (5′–3′)
Chka	NM_013490	CAGGGGTGGTCTCAGTAACAT	GTCGGCCTTGGGGAAAGATG
Cyp2a12	NM_133657	TGGGGAACGAGCCAAACAAC	CGCCGAAGACAATGGAGCTA
Cyp2c38	NM_010002	ACAGGCAAACCACATCGAACA	GCTACGGTGTCTACCAACCAC
Elovl3	NM_007703	GTCGTCTATCTGTTGCTCATCG	TGCAGCCCAACTTTCAACAAG
Pik3c2g	NM_207683	CCATCTATCAGCTAATCGACGTG	GGAACACACTGTGAAGCTCAG
Insig2	NM_133748	GGAGTCACCTCGGCCTAAAAA	CAAGTTCAACACTAATGCCAGGA
Ppp1r3c	NM_016854	TGATCCATGTGCTAGATCCACG	ACTCTGCGATTTGGCTTCCTG
Ptgds	NM_008963	TGCAGCCCAACTTTCAACAAG	TGGTCTCACACTGGTTTTTCCT
Gapdh	NM_001001303	CGGTGCTGAGTATGTCG	TTCTGGGTGGCAGTGAT

Note. NCBI RefSeq, National Center for Biotechnology Information Reference Sequence.

and Avadis 4.3 (Strand Life Sciences, India) software applied when unspecified. For further analysis, gene sets with different dose and time effects according to two-way ANOVA were classified into time-dependent, dose-dependent, and combined effect (i.e., both time- and dose-dependent, MTD) groups. The three groups were then classified into with- and without-interaction groups according to the significance of the interaction terms under saturated linear models.

Quantitative real-time polymerase chain reaction. Total RNA was prepared using the Easy-Blue total RNA extraction kit (Intron Biotech), and single-strand cDNA was synthesized from the RNA in a reaction mixture containing random hexamers and Superscript II reverse transcriptase (Invitrogen, Carlsbad, CA). Gene-specific primers designed using Oligo 6.0 software (Molecular Biology Insights, Cascade, CO) were used (Table 1). Quantitative real-time polymerase chain reaction (qRT-PCR) amplifications were performed using Fast Start DNA Master SYBR Green I Mixture Kit (Roche Diagnostics, Mannheim, Germany) in a Light Cycler system (Roche Diagnostics) following manufacturer's protocol. To determine the specificity of amplification, melting curve analysis was applied to all final PCR products.

RESULTS

Clinical Chemistry and Histological Endpoints

Treatment of ICR mice with 0.1 or 1 g/kg tetracycline did not change the level of plasma ALT activity in any of the animals (Fig. 2A). In the histological analysis, no biologically

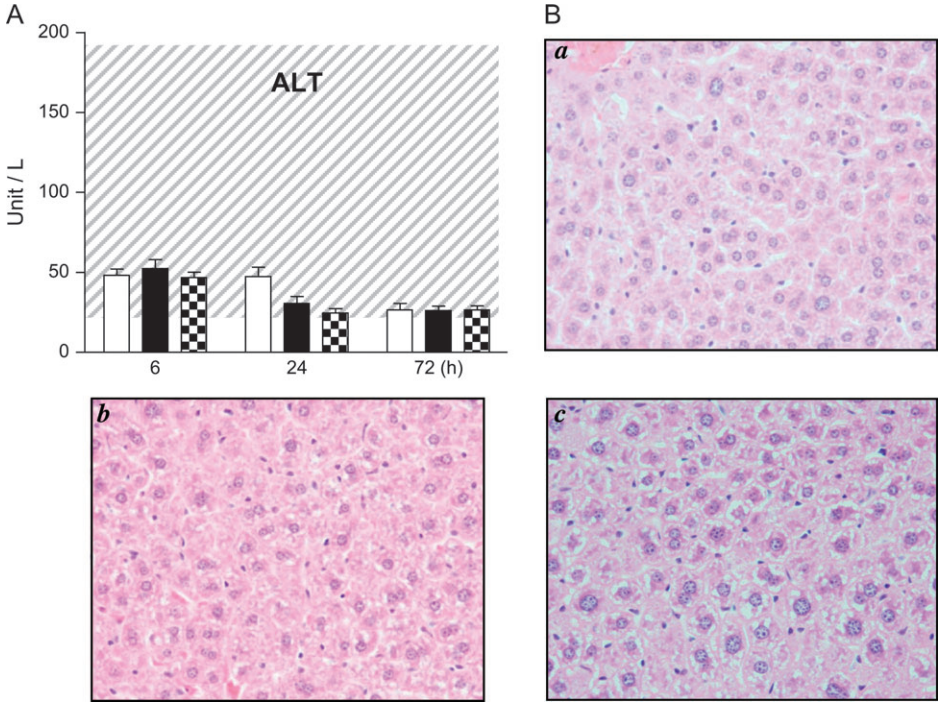

FIG. 2. Biochemical and pathological analysis of the serum and liver obtained from ICR mice after oral exposure to tetracycline. (A) The levels of serum ALT were measured at each time point in vehicle (open bar), low-dose (filled bar), and high-dose (checked bar) treatment groups. Dashed line indicates the normal range of ALT level in ICR mice. Results are mean ± SD of three mice. (B) Histopathological analysis of hematoxylin-eosin–stained paraffin sections from (a) C24, (b) L24, and (c) H24 liver samples (×400).

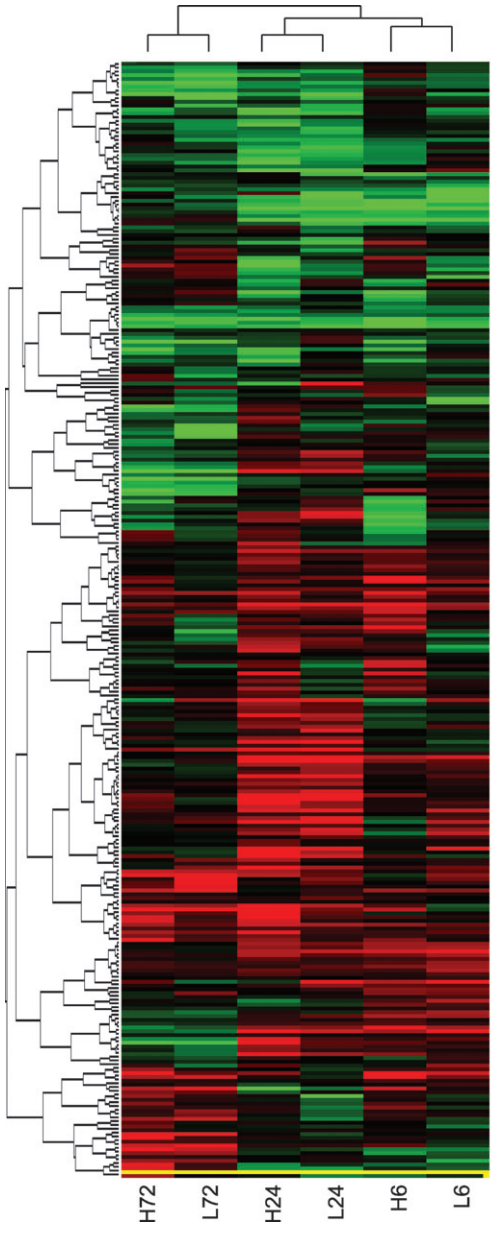

FIG. 3. Hierarchical clustering analysis of differentially expressed genes in tetracycline-treated mice liver. Hierarchical clustering analysis was performed with 298 genes that were obtained by the adjustment of the data using Benjamini-Hochberg multiple test correction. Red color and green color in matrix indicate the relative gene induction and repression, respectively. Dendrograms of each group (above the matrix) and probe sets (left of the matrix) represent the overall similarities in gene expression profiles.

significant liver damage was observed at 6 or at 72 h after treatment (data not shown). However, high-dose tetracycline at 24 h caused histological lesions including microvesicular steatosis, which is characterized by the presence of numerous small vesicles of fat that do not displace the nucleus (Fig. 2B). Other serum biomarkers tested in this study were not changed significantly by the drug treatment, indicating that the treatment condition used in this study did not induce any serious lesions.

Global Gene Expression Analysis Following Tetracycline Treatment

A total of 27 Applied Biosystems Mouse Genome Survey Microarrays were used to analyze global gene expression changes in mouse liver exposed to vehicle or to tetracycline (0.1 or 1 g/kg) at 6, 24, and 72 h posttreatment. Two-way ANOVA of the dose- and time-response data identified 4934 genes (from a total of 32,381 probe sets) that showed statistically significant changes in expression ($p < 0.05$, Supplementary data 1). Functional categorization of the data was performed using the annotation information in the PANTHER database for ontology. Tetracycline-induced changes in expression of genes involved in a variety of biological processes. The largest group of genes was those associated with signal transduction, while genes of nucleic acid metabolism, protein metabolism, and developmental processes were the next most abundant annotation groups. Tree analysis of the genes classified patterns of relative responses for all treatment conditions relative to controls (Fig. 3). The greatest distance between nodes was between the L6 and the H72 groups. Low- and high-dose groups at each time point were in the same node, and the distances between nodes increased in response to the time of treatment, indicating a stronger effect of time than dose in our experimental regimen. Further classification of the results into four groups under the terms of a saturated linear model demonstrated that 3229 of 4934 differentially expressed genes showed a time-dependent response, and only 667 genes were dose dependent. These results again show that the effect of time on differential gene expression was more significant than that of dose in our tetracycline-induced gene expression analysis.

Adjustment of the data by the Benjamini-Hochberg multiple testing correction (Benjamini and Hochberg, 1995) reduced the number of affected genes to 298 (Supplementary data 2), and the expression of a total 96 genes was found to be changed by more than twofold (up or down) by at least one treatment condition. Functional categorization of the genes using the PANTHER database for ontology is presented in Table 2. Genes without clear annotations, such as expressed sequence tags, were excluded from the table.

Expression of Genes in Lipid Metabolism

We next investigated the expression of genes known to be involved in lipid metabolism. The whole data set obtained from each treatment group was analyzed by two-sample Student's *t*-test against that from the corresponding vehicle control group. In general, genes were more likely to be induced than repressed by tetracycline treatment. The greatest number of changes in gene expression occurred at 24 h, when signals from 2429 genes in the high-dose (H24) group and 1009 genes in the low-dose (L24) group were changed. Protein tyrosine phosphatase receptor type C and the RIKEN cDNA

TABLE 2
Genes Altered More than Twofold (two-way ANOVA; $p < 0.05$) Compared with Control in the Liver of Mice Given Tetracycline

		Low dose (0.1 g/kg)			High dose (1 g/kg)		
Gene symbol	Grip query	6 h	24 h	72 h	6 h	24 h	72 h
Cell adhesion							
Pcdh18	NM_130448	0.73	− 0.08	0.34	1.02	− 0.29	− 0.42
Lrrc4b	NM_198250	0.59	− 0.21	− 0.25	0.48	0.93	− 1.08
Itgae	NM_008399	0.47	− 0.56	− 0.32	0.51	− 1.16	0.84
Cell proliferation and differentiation							
Jag1	NM_013822	0.43	1.53	0.14	0.46	0.44	0.03
Pcdh18	NM_130448	0.73	− 0.08	0.34	1.02	− 0.29	− 0.42
Jak1	NM_146145	0.30	− 0.19	− 0.28	− 1.31	− 0.29	− 0.40
1200009B18Rik	NM_026168	0.28	− 0.30	− 0.20	− 1.17	− 0.35	0.11
Mal	NM_010762	− 0.45	− 1.23	1.61	− 0.52	− 0.56	0.46
Ccnb3	NM_183015	− 1.63	0.20	1.37	− 0.47	2.00	1.16
Prlpc2	NM_023332	0.95	0.02	1.31	1.25	0.20	− 0.12
Developmental process							
Zic5	NM_022987	− 0.11	0.60	− 0.75	− 1.32	0.88	− 0.50
Rps6ka2	NM_011299	− 0.71	− 0.74	0.30	− 0.82	− 1.07	0.80
Sema6d	NM_199240	1.34	0.39	− 0.99	1.67	0.99	0.04
Gata2	NM_008090	− 0.08	0.62	− 0.66	− 0.10	− 0.17	− 1.11
9430095K15Rik	AK035166	0.47	0.40	0.18	1.37	0.41	− 1.14
Jag1	NM_013822	0.43	1.53	0.14	0.46	0.44	0.03
Pcdh18	NM_130448	0.73	− 0.08	0.34	1.02	− 0.29	− 0.42
Csf1	M21149	0.24	0.18	− 0.12	0.84	1.33	− 0.02
Jak1	NM_146145	0.30	− 0.19	− 0.28	− 1.31	− 0.29	− 0.40
Mal	NM_010762	− 0.45	− 1.23	1.61	− 0.52	− 0.56	0.46
2700038E08Rik	NM_197993	0.10	− 0.00	− 0.11	− 1.67	0.09	− 0.05
Prlpc2	NM_023332	0.95	0.02	1.31	1.25	0.20	− 0.12
Immunity and defense							
Jag1	NM_013822	0.43	1.53	0.14	0.46	0.44	0.03
Csf1	M21149	0.24	0.18	− 0.12	0.84	1.33	− 0.02
Mal	NM_010762	− 0.45	− 1.23	1.61	− 0.52	− 0.56	0.46
Lrrc4b	NM_198250	0.59	− 0.21	− 0.25	0.48	0.93	− 1.08
Intracellular protein traffic							
Gga1	NM_145929	0.28	− 0.26	− 0.66	2.07	− 0.43	− 0.31
Stam	NM_011484	0.11	0.60	− 0.56	− 1.10	1.083	− 0.20
Mal	NM_010762	− 0.45	− 1.23	1.616	− 0.51	− 0.56	0.46
9530019H02Rik	NM_198163	− 0.00	0.08	− 0.426	− 1.73	0.25	− 0.35
Lipid, fatty acid, and steroid metabolism							
Auh	NM_016709	− 0.33	0.15	0.20	− 1.48	− 0.13	0.30
Hadha	NM_178878	0.51	0.78	− 0.26	− 1.80	0.57	− 0.53
Sult2b1	NM_017465	0.69	− 0.56	− 0.30	0.40	1.07	− 0.90
C130053K05Rik	NM_175467	− 0.02	0.70	0.76	2.64	0.08	0.14
Nucleoside, nucleotide, and nucleic acid metabolism							
Zic5	NM_022987	− 0.11	0.60	− 0.75	− 1.32	0.88	− 0.50
Gata2	NM_008090	− 0.08	0.62	− 0.66	− 0.10	− 0.17	− 1.11
Jag1	NM_013822	0.43	1.53	0.14	0.46	0.44	0.03
Exosc10	NM_016699	0.33	0.12	0.01	− 1.89	0.09	− 0.05
D030046N04Rik	AK017405	~ 0.32	0.57	0.74	− 1.66	0.82	0.48
Pde4b	NM_019840	0.46	2.25	− 1.13	− 1.26	1.40	− 1.81
Exosc9	NM_019393	0.36	1.80	0.22	0.51	0.40	0.12
Pabpc2	NM_011033	0.83	2.27	0.95	1.58	0.31	0.47
Dhx29	NM_172594	1.04	2.35	− 0.77	1.71	1.02	− 0.63
Npm2	NM_181345	0.39	0.41	0.63	0.27	1.70	− 0.15
Gmpr2	NM_134075	0.13	0.42	− 0.03	− 1.27	0.07	− 0.51
Cbfa2t2h	NM_172860	0.18	− 0.80	1.30	− 0.24	0.17	0.20
Polr2a	NM_009089	0.37	0.15	− 0.70	1.02	− 0.31	− 0.53
2700038E08Rik	NM_197993	0.10	− 0.00	− 0.11	− 1.67	0.09	− 0.05

TABLE 2—*Continued*

Gene symbol	Grip query	Low dose (0.1 g/kg) 6 h	24 h	72 h	High dose (1 g/kg) 6 h	24 h	72 h
Arnt	NM_009709	0.63	0.85	− 0.66	− 0.92	1.05	− 0.78
Hist2h4	NM_033596	− 0.04	− 0.87	− 0.40	− 1.32	− 1.52	− 0.11
Zfp312	NM_080433	0.39	− 0.05	− 1.27	− 0.12	1.83	− 0.46
Protein metabolism and modification							
Rps6ka2	NM_011299	− 0.71	− 0.74	0.30	− 0.82	− 1.07	0.80
Gga1	NM_145929	0.28	− 0.26	− 0.66	2.07	− 0.43	− 0.31
Rpl23	AK002579	0.07	− 0.77	0.05	− 1.33	− 0.59	0.30
C920001D21Rik	NM_177081	− 0.41	0.79	1.27	1.78	0.57	1.90
Jak1	NM_146145	0.30	− 0.19	− 0.28	− 1.31	− 0.29	− 0.40
Pak2	NM_177326	0.25	− 0.44	0.98	0.63	0.98	1.32
Mrps12	NM_011885	− 0.17	− 0.76	0.12	− 1.76	− 0.88	0.21
Dnajb8	NM_019964	1.42	0.97	− 0.94	1.68	0.32	− 1.34
Hadha	NM_178878	0.51	0.78	− 0.26	− 1.80	0.57	− 0.53
Ttc1	NM_133795	0.31	− 0.10	− 0.04	− 1.16	− 0.05	0.20
Sensory perception							
Olfr493	NM_146310	0.04	0.33	− 0.00	1.00	− 0.38	− 1.55
Olfr976	NM_146367	− 0.36	0.71	0.85	2.74	0.51	− 0.18
Pomc1	NM_008895	0.04	0.33	− 1.22	1.87	− 0.34	− 0.86
Kera	NM_008438	0.56	− 0.40	− 1.67	1.49	− 0.58	− 0.50
Transport							
Pkd1l3	NM_181544	0.58	− 0.97	0.056	0.21	− 1.32	− 0.24
Cacna2d1	NM_009784	− 0.36	1.08	− 0.62	0.49	0.27	− 0.18
Slc1a4	NM_018861	0.51	0.51	0.97	0.83	2.08	0.46
Fxyd7	NM_022007	− 0.77	− 0.56	1.35	1.36	0.49	0.73
Slc25a30	AK090086	− 0.27	0.01	− 0.31	0.42	− 0.17	− 1.12
Carbohydrate metabolism							
1700007H16Rik	NM_027945	0.28	1.30	− 0.93	− 0.67	1.15	− 0.72
Auh	NM_016709	− 0.33	0.15	0.20	− 1.47	− 0.13	0.30
Ppp1r3c	NM_016854	0.75	2.73	− 0.53	− 0.93	2.83	− 0.77
Hadha	NM_178878	0.51	0.78	− 0.26	− 1.79	0.57	− 0.53
Signal transduction							
Gpr151	AK048591	− 0.23	0.18	− 0.90	0.25	− 0.062	− 1.22
Pkd1l3	NM_181544	0.57	− 0.97	0.06	0.21	− 1.32	− 0.24
Olfr493	NM_146310	0.04	0.33	− 0.00	1.00	− 0.38	− 1.55
Olfr976	NM_146367	− 0.36	0.71	0.85	2.74	0.51	− 0.18
Rps6ka2	NM_011299	− 0.71	− 0.74	0.30	− 0.82	− 1.07	0.80
Sema6d	NM_199240	1.34	0.39	− 0.99	1.67	0.95	0.04
9430095K15Rik	AK035166	0.47	0.40	0.18	1.37	0.41	− 1.14
Ctgf	NM_010217	− 0.78	0.02	0.29	− 1.21	0.85	0.40
Cacna2d1	NM_009784	− 0.36	1.08	− 0.63	0.49	0.27	− 0.18
Slc1a4	NM_018861	0.50	0.51	0.97	0.83	2.08	0.46
Pcdh18	NM_130448	0.73	− 0.08	0.34	1.02	− 0.29	− 0.42
Csf1	M21149	0.24	0.18	− 0.12	0.84	1.33	− 0.02
C920001D21Rik	NM_177081	− 0.41	0.79	1.27	1.78	0.57	1.90
Jak1	NM_146145	0.30	− 0.19	− 0.28	− 1.31	− 0.29	− 0.40
Fxyd7	NM_022007	− 0.77	− 0.56	1.35	1.36	0.49	0.73
Pde4b	NM_019840	0.46	2.25	− 1.13	− 1.24	1.39	− 1.81
Stam	NM_011484	0.11	0.59	− 0.55	− 1.10	1.08	− 0.20
Pomc1	NM_008895	0.04	0.33	− 1.22	1.87	− 0.34	− 0.86
Mal	NM_010762	− 0.45	− 1.23	1.61	− 0.52	− 0.56	0.46
Kera	NM_008438	0.56	− 0.40	− 1.67	1.49	− 0.58	− 0.50
Rapgef5	NM_175930	− 0.26	0.99	0.08	1.13	− 0.11	0.07
Lrrc4b	NM_198250	0.59	− 0.21	− 0.25	0.48	0.93	− 1.08
Prlpc2	NM_023332	0.95	0.02	1.31	1.25	0.20	− 0.12

Note. Values represent fold changes on $\log_2$ scale compared with corresponding vehicle control. Grip: Grid Resources Information Protocol.

TABLE 3
Significantly Upregulated Genes (Student's *t*-test; $p < 0.05$) in H24 Compared with C24, Which Are Involved in Lipid Metabolism (fold change $\geq$ 1.5)

Gene symbol	Grip query	Fold change	Gene symbol	Grip query	Fold change	Gene symbol	Grip query	Fold change
Elovl3	NM_007703	3.10	*Pik3cb*	NM_029094	1.04	*Cyp2j9*	NM_028979	0.75
Cyp2c38	NM_010002	2.93	*Cyp2d13*	NM_133695	1.01	*Faah*	NM_010173	0.75
Cyp2c39	NM_010003	2.46	*Acbd5*	NM_028793	0.99	*Cyp21a1*	NM_009995	0.74
Cyp2c37	NM_010001	2.34	*2810007J24Rik*	NM_175250	0.96	*Pik4cb*	NM_175356	0.73
Prkab2	NM_182997	2.32	*2310076L09Rik*	NM_025874	0.96	*Srebf1*	NM_011480	0.72
Pik3c2g	NM_207683	2.11	*2410051C13Rik*	NM_145401	0.95	*Pitpn*	NM_008850	0.71
Cyp2a12	NM_133657	2.11	*Pld1*	NM_008875	0.95	*Sec14l4*	NM_146013	0.71
Chka	NM_013490	2.05	*Nsdhl*	AK088026	0.95	*D6Ucla1e*	NM_197985	0.71
Ptgds	NM_008963	2.02	*Abcd3*	NM_008991	0.94	*Inpp5f*	NM_178641	0.70
BC031140	BC024424	1.80	*Siat4c*	NM_009178	0.94	*Aoah*	AK015300	0.70
1700020G04Rik	NM_198414	1.75	*Hsd3b6*	NM_013821	0.94	*AI313915*	NM_144845	0.70
Sult5a1	NM_020564	1.74	*Acsl1*	NM_007981	0.93	*1810044O22Rik*	NM_025558	0.69
Akr1d1	NM_145364	1.70	*Cat*	NM_009804	0.93	*Agpat2*	NM_026212	0.68
Pik3c2a	NM_011083	1.66	*Elovl6*	NM_130450	0.92	*Pik3ca*	NM_008839	0.68
Crot	NM_023733	1.64	*Cyp4f18*	NM_024444	0.90	*AI746432*	NM_207216	0.67
Plg	NM_008877	1.60	*Nr2e3*	NM_013708	0.89	*Acadsb*	NM_025826	0.67
BC051083	NM_181409	1.57	*Hsd3b2*	NM_153193	0.89	*Acox1*	NM_015729	0.67
Rxrg	NM_009107	1.49	*9530058O11Rik*	AK031448	0.89	*Hsd17b1*	NM_010475	0.67
Plcz1	NM_054066	1.36	*4632417N05Rik*	NM_028725	0.88	*Sptlc1*	NM_009269	0.67
Plcg1	NM_021280	1.34	*Ugcg*	NM_011673	0.85	*Hsd3b4*	NM_008294	0.66
Pip5k1a	AK077334	1.30	*Mgat2*	NM_146035	0.83	*Tra1*	NM_011631	0.66
Neu3	NM_016720	1.29	*Insig2*	NM_133748	0.83	*Pcx*	NM_008797	0.66
Hmgcs1	NM_145942	1.24	*Abca1*	NM_013454	0.81	*Hsd17b2*	NM_008290	0.65
Cyp51	NM_020010	1.22	*Gba2*	NM_172692	0.80	*Cyp8b1*	NM_010012	0.64
Hsd3b7	NM_133943	1.21	*Cyp4f14*	NM_022434	0.80	*Pip5k1b*	NM_008847	0.64
Cyp7a1	NM_007824	1.20	*CRAD-L*	NM_145424	0.79	*2010321J07Rik*	NM_028094	0.64
Hexb	NM_010422	1.17	*Siat4a*	NM_009177	0.79	*Pten*	NM_008960	0.63
Lass5	NM_028015	1.13	*Sdro*	NM_027301	0.78	*Abca8b*	NM_013851	0.62
Spp1	NM_009263	1.11	*Rnpep*	NM_145417	0.77	*Sacm1l*	NM_030692	0.61
Cyp2c70	NM_145499	1.11	*Acat2*	NM_009338	0.77	*Plscr4*	NM_178711	0.60
Elovl5	NM_134255	1.08	*Cyp2j5*	NM_010007	0.75	*Pecr*	NM_023523	0.59
Sult2b1	NM_017465	1.07	*Gpd2*	NM_010274	0.75	*Lass2*	NM_029789	0.59

Note. Values represent fold changes on $\log_2$ scale compared with corresponding vehicle control.

8430438D04 were upregulated at all three time points. Lipid metabolism–related genes were present in the high- and low-dose gene groups (141 and 62, respectively; Tables 3 and 4). As shown in Figure 4, the overall net effects of altered gene expression associated with lipid metabolism were to increase cholesterol and TG biosynthesis and to decrease β-oxidation of fatty acid.

Validation of Microarray Data

Microarray results were confirmed for a subset of genes using qRT-PCR. In general, the results obtained from microarray experiments correlated well with qRT-PCR. For simple validation, 12 genes were verified by qRT-PCR, all of which displayed expression patterns comparable with the microarray data (Table 5). Because the steatosis was induced only in H24 group and was apparently reversed between 24 and 72 h, we analyzed the data by Tukey's *post hoc* test to find the genes that were upregulated in H24 and downregulated in H72. There was good agreement in the magnitude of the fold change when comparing microarray and qRT-PCR data, except for Myt1L that showed discrepancy between the two methods. These genes represent steatosis-associated injury and recovery specific genes (Fig. 5).

DISCUSSION

Tetracycline is a widely used broad-spectrum antibiotic that is known to induce microvesicular steatosis in the liver. Although the hepatotoxic effect of tetracycline is evident, and is severe and even fatal in some vulnerable patients, a systematic approach to identifying a toxicity mechanism has not yet been applied. In the present study, we investigated the temporal and dose-dependent effects of acute tetracycline on hepatic gene expression, using high-density oligonucleotide microarrays, with special emphasis on the genes associated with lipid metabolism. The goals of this study were (1) to

TABLE 4
Significantly Downregulated Genes (Student's *t*-Test; $p < 0.05$) in H24 Compared with C24, Which Are Involved in Lipid Metabolism (fold change $\geq$ 1.5)

Gene symbol	Grip query	Fold change	Gene symbol	Grip query	Fold change	Gene symbol	Grip query	Fold change
2810004N20Rik	NM_025576	− 0.59	*Bzrp*	NM_009775	− 0.77	*4921521F21Rik*	NM_027582	− 1.14
Arsa	NM_009713	− 0.59	*Osbpl8*	NM_175489	− 0.79	*Pla2g2a*	NM_011108	− 1.19
Crat	NM_007760	− 0.59	*Cyp46a1*	NM_010010	− 0.80	*Sorl1*	NM_011436	− 1.24
Mir16	NM_019580	− 0.59	*Atp11a*	NM_175220	− 0.83	*Lrp4*	NM_172668	− 1.28
Rdh6	NM_009040	− 0.59	*Mpra*	NM_027995	− 0.86	*Fabp1*	NM_017399	− 1.28
Dpm1	NM_010072	− 0.61	*Cyp26a1*	NM_007811	− 0.87	*Ar*	NM_013476	− 1.30
Fdx1	NM_007996	− 0.66	*Ndufab1*	BC053970	− 0.87	*Dci*	NM_010023	− 1.33
Keg1	NM_029550	− 0.66	*Cyb5*	NM_025797	− 0.88	*Pik3cd*	NM_008840	− 1.66
Dgka	NM_016811	− 0.69	*2610020H15Rik*	NM_025638	− 0.92	*Cyp17a1*	NM_007809	− 1.81
Cyp3a44	NM_177380	− 0.69	*Dbi*	NM_007830	− 0.93	*Agpat4*	NM_026644	− 1.90
Gpx3	NM_008161	− 0.69	*Gpx4*	NM_008162	− 1.02	*Pla2g2d*	NM_011109	− 2.21
Fabp4	NM_024406	− 0.70	*Thrsp*	NM_009381	− 1.05	*Pctp*	BC071234	− 2.27
Cyp2a5	NM_007812	− 0.72	*Cyp2a4*	NM_009997	− 1.05	*Pip5k2b*	NM_054051	− 2.28
Apoc3	NM_023114	− 0.72	*Apoc2*	NM_009695	− 1.07	*Osbpl3*	NM_027881	− 2.52
Apoc1	NM_007469	− 0.76	*Alox5ap*	NM_009663	− 1.10	*Fabp7*	NM_021272	− 3.07

Note. Values represent fold changes on $\log_2$ scale compared with corresponding vehicle control.

investigate the effects of tetracycline on global gene expression, in order to develop biomarkers and (2) to identify genes that are involved in the steatogenic action of tetracycline, in order to elucidate its mode of toxicity.

Tetracycline-Induced Global Gene Expression Changes

Accumulating evidence has demonstrated that microarray technology for global gene expression profiling is a powerful tool in toxicological research, especially in the field of predictive toxicogenomics. A critical hypothesis in this research area is that the resulting transcript profile can provide both reliable advance information on possible toxic outcomes and mechanistic insight into the toxicity itself. To use short-term toxicogenomic data in predicting results of longer duration studies, a database of compounds with known chronic toxicity must be developed. Although many technical problems

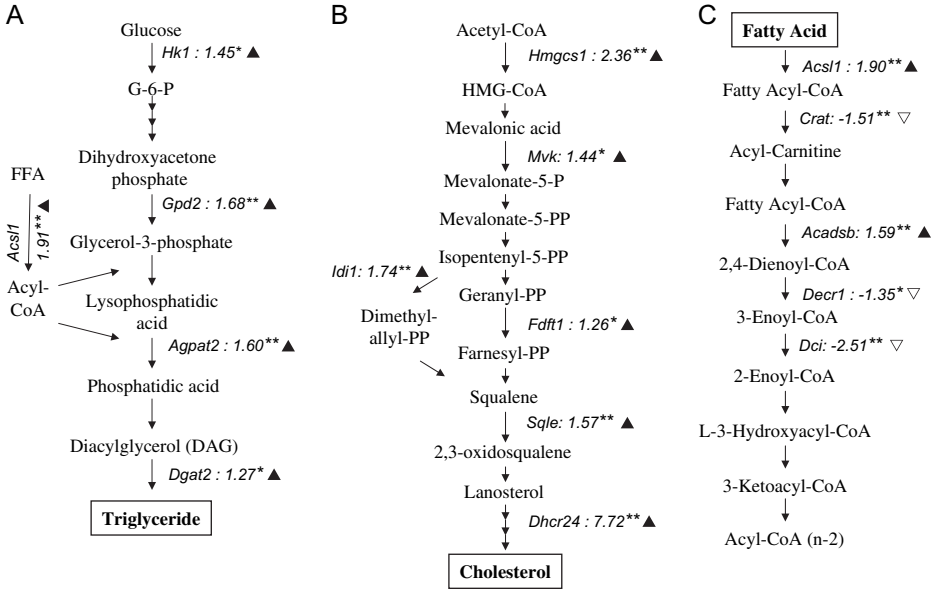

FIG. 4. Pathways for major lipid metabolism (TG [A], cholesterol biosynthesis [B], and β-oxidation of fatty acid [C]) and the relative induction or repression of the genes, being statistically different from vehicle control based on a two-sample Student's *t*-test. To make data more intelligible, they are presented as fold induction in natural numbers (not in $\log_2$ scale). (**$p < 0.05$ and fold induction or repression $\geq$ 1.5; *$p < 0.05$ and fold induction or repression $\geq$ 1.25).

TABLE 5
qRT-PCR Validation of Selected Genes from Microarray Data in L24 and H24 Groups

Gene		Microarray	qRT-PCR
Chka	L24	2.33 ± 0.26	1.59 ± 0.01
	H24	2.05 ± 0.01	1.87 ± 0.40
Cyp2a12	L24	0.99 ± 0.54	3.59 ± 0.73
	H24	2.11 ± 0.02	2.34 ± 0.84
Cyp2c38	L24	1.84 ± 0.32	2.70 ± 0.10
	H24	2.93 ± 0.06	1.98 ± 0.86
Elovl3	L24	2.55 ± 0.83	2.32 ± 0.42
	H24	3.10 ± 0.11	1.12 ± 0.52
Pik3c2g	L24	1.65 ± 0.41	2.28 ± 0.13
	H24	2.11 ± 0.06	1.54 ± 0.04
Insig2	L24	1.48 ± 0.33	3.17 ± 0.09
	H24	0.83 ± 0.00	1.77 ± 0.69
Ppp1r3c	L24	2.73 ± 0.24	2.97 ± 0.79
	H24	2.83 ± 0.06	2.44 ± 0.13
Ptgds	L24	2.23 ± 0.44	2.41 ± 0.37
	H24	2.02 ± 0.01	2.43 ± 0.51

Note. Data are mean ± SD of three independent measurements, which represent fold change on $\log_2$ scale compared with data obtained from C24 group.

limit the usefulness of the concept at present, pattern recognition experiments may hold considerable promise (Hamadeh *et al.*, 2002). For this purpose, the Korean Toxicogenomic Research Consortium has embarked on a project to construct a toxicogenomic database of known hepatotoxicants, including tetracycline as a steatogenic drug.

When the microarray data from our nine experimental groups were analyzed statistically using two-way ANOVA, about 15% (4934 of 32,381) of the genes were significantly affected by tetracycline—a relatively large subset. To determine the dominant factor influencing the gene expression pattern, we next classified and adjusted the data using gene tree analysis, a saturated linear model, and the Benjamini-Hochberg multiple testing correction. When thousands of hypotheses are tested simultaneously, the chance of detecting false positives increases, and multiple testing methods should be applied to assess the statistical significance of findings. To control for the false discovery rate (FDR), defined as the expected proportion of false positives among the genes with significant expression changes, we applied the Benjamini-Hochberg multiple testing correction method. In the present study, the estimated number of false positives was presumed to be about 15 out of 298 genes (FDR < 0.05). The combined results of the three methods of analysis indicate unequivocally that the effect of time on differential gene expression is more significant than that of dose in tetracycline-induced gene expression.

Tetracycline-Induced Changes in Lipid Metabolism

The typical phenotypic change induced by tetracycline is fatty liver. We analyzed data from each treatment group against the corresponding vehicle control. Only at 24 h was the number of genes induced or suppressed directly proportional to the tetracycline dose. At that time point, of 1009 and 2429 genes that were changed by more than 1.5-fold in the low- and high-dose groups, respectively, 62 and 141 genes were involved in lipid metabolism, including mitochondrial and peroxisomal β-oxidation of free fatty acid, TG synthesis, and cholesterol synthesis.

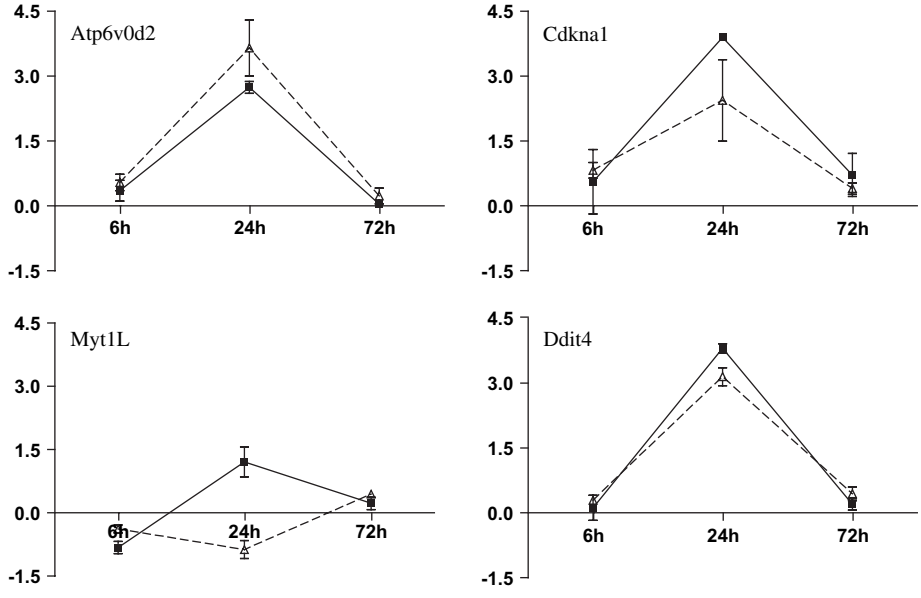

FIG. 5. Real-time PCR validation of the genes that were upregulated in H24 and downregulated in H72, which represent directional changes in the steatosis-associated injury and recovery specific genes. Data represent fold change on $\log_2$ scale compared with the corresponding control group.

Mechanisms so far reported by which tetracycline induces steatosis include the inhibition both of β-oxidation of free fatty acids and of lipoprotein secretion from the liver (Freneaux *et al.*, 1988; Letteron *et al.*, 2003). However, the effect of tetracycline on TG and cholesterol synthesis is not known. We observed altered patterns of expression for genes involved in these synthetic pathways. Glycerol-3-phosphate dehydrogenase (*Gpd2*) catalyzes the reduction of dihydroxyacetone phosphate to glycerol-3-phosphate, which is in turn acylated by glycerol-3-phosphate-acyltransferase and acylglycerol-phosphate-acyltransferase (*Agpat2*) to give phosphatidic acid. Phosphatidic acid is hydrolyzed to diacylglycerol, and the third acyl group is introduced by diacylglycerol acyltransferase (*Dgat2*) to form a TG. The reaction partner in all acylation reactions, fatty acyl-CoA, is synthesized by acyl-CoA synthase (*Acsl1*). In the current study, we found significant increases in expression of many genes implicated in TG synthesis (*Gpd2*, *Agpat2*, and *Acsl1*). A change in *Dgat2* expression was also statistically significant but reflected an increase of only 27%. As a result of these changes in expression, serum TG concentrations in tetracycline-treated mice were increased significantly. Studies have demonstrated that a significant increase in acylglycerol-phosphate-acyltransferase activity by overexpression of the *Agpat1* gene (Ruan and Pownall, 2001) increases TG synthesis, and a decrease in *Agpat1* activity by mutation (Gangar *et al.*, 2002) in adipocytes leads to decreased production of TGs. Thus, upregulation of genes involved in TG synthesis is a response that can lead to tetracycline-induced fat accumulation in the liver (Fig. 4A).

Cholesterol synthesis occurs in four phases: the synthesis of mevalonic acid from acetate, the conversion of mevalonic acid into isoprene units, the polymerization of isoprene units to squalene, and further processing to cholesterol. We found that tetracycline affects several genes in each steps of the cholesterol biosynthetic pathway. They include Hmgcs1 for the synthesis of HMG-CoA, *Mvk* for the phosphorylation of mevalonic acid, and Fdft1 for the formation of farnesyl diphosphate.

Sqle, encoding an enzyme adding one oxygen atom to the end of the squalene chain, is regulated by the cholesterol pool in the body. Cholesterol feeding reduced hepatic *Sqle* activity to inhibit synthesis of redundant cholesterol (Satoh *et al.*, 1990). Similarly, a specific inhibitor of *Sqle* suppressed the secretion of cholesterol (Horie *et al.*, 1993). Cell and animal models with decreased expression of 24-dehydrocholesterol reductase (*Dhcr24*) exhibit decreased cholesterol synthesis, and mutations in the *Dhcr24* gene cause a cholesterol biosynthesis disorder (Waterham *et al.*, 2001). In mice with a targeted disruption of *Dhcr24*, plasma and tissues contain almost no cholesterol, and desmosterol was shown to account for 99% of total sterols (Wechsler *et al.*, 2003). Thus, tetracycline induction of *Hmgcs1*, *Mvk*, *Idi1*, *Fdft1*, *Sqle*, and *Dhcr24* would facilitate increased hepatic cholesterol synthesis and a resultant fatty liver (Fig. 4B).

Mitochondrial β-oxidation is a major process in fatty acid degradation. Although the first step is the conversion of fatty acid into fatty acyl-CoA by acyl-CoA synthase (*Acsl1*), the rate-limiting step is the transport of fatty acyl-CoA through the mitochondrial membrane via fatty acylcarnitine, catalyzed by carnitine acyltransferase (*Crat*). Tetracycline downregulated the expression of *Crat1* and of 2,4-dienoyl-CoA reductase 1 (*Decr1*) and dodecenoyl-CoA delta isomerase (*Dci*), which play pivotal roles in mitochondrial β-oxidation (Fig. 4C). Similarly, many other chemicals that induce fatty liver have also been reported to influence fatty acid metabolism (Guruge *et al.*, 2006; Richards *et al.*, 2004). Lipid catabolism is also mediated via microsomal ω-oxidation catalyzed by the *Cyp4f* family of enzymes (Le Quere *et al.*, 2004; Sanders *et al.*, 2005). Upregulation of *Cyp4f14* and *Cyp4f18* by tetracycline in our study suggests that the β-oxidation pathway is inadequate to deal with the lipid accumulation induced by tetracycline, and a greater capacity for ω-oxidation is needed to increase the breakdown of hepatic lipids.

In summary, we documented a global gene expression profile for mouse liver following acute tetracycline treatment, as determined on oligonucleotide microarrays. We found that tetracycline affects gene expression associated with lipid metabolism in a direction to increase TG and cholesterol biosynthesis and decrease β-oxidation of fatty acids. These results contribute not only to produce a database that can be used for prediction of toxicity through pattern recognition but also to our understanding of the mechanism of tetracycline-induced steatogenic hepatotoxicity.

ACKNOWLEDGMENTS

This work was supported by a grant from Korea Food and Drug Administration (KFDA-05122-TGP-584).

REFERENCES

Amacher, D. E., and Martin, B. A. (1997). Tetracycline-induced steatosis in primary canine hepatocyte cultures. *Fundam. Appl. Toxicol.* **40,** 256–263.

Ballet, F. (1997). Hepatotoxicity in drug development: Detection, significance and solutions. *J. Hepatol.* **26**(Suppl. 2), 26–36.

Benjamini, Y., and Hochberg, Y. (1995). Controlling the false discovery rate: A practical and powerful approach to multiple testing. *J. R. Stat. Soc. B* **57,** 289–300.

Bhagavan, B. S., Wenk, R. E., McCarthy, E. F., Gebhardt, F. C., and Lustgarten, J. A. (1982). Long-term use of tetracycline. *JAMA* **247,** 2780.

Bolstad, B. M., Irizarry, R. A., Astrand, M., and Speed, T. P. (2003). A comparison of normalization methods for high density oligonucleotide array data based on variance and bias. *Bioinformatics* **19,** 185–193.

Freneaux, E., Labbe, G., Letteron, P., The, L. D., Degott, C., Geneve, J., Larrey, D., and Pessayre, D. (1988). Inhibition of the mitochondrial oxidation of fatty acids by tetracycline in mice and in man: Possible role in microvesicular steatosis induced by this antibiotic. *Hepatology* **8,** 1056–1062.

Gabler, W. L., Smith, J., and Tsukuda, N. (1992). Comparison of doxycycline and a chemically modified tetracycline inhibition of leukocyte functions. *Res. Commun. Chem. Pathol. Pharmacol.* **78,** 151–160.

Gangar, A., Raychaudhuri, S., and Rajasekharan, R. (2002). Alteration in the cytosolic triacylglycerol biosynthetic machinery leads to decreased cell growth and triacylglycerol synthesis in oleaginous yeast. *Biochem. J.* **365,** 577–589.

Guruge, K. S., Yeung, L. W. Y., Yamanaka, N., Miyazaki, S., Lam, P. K. S., Giesy, J. P., Jones, P. D., Yamashita, N. (2006). Gene expression profiles in rat liver treated with perfluorooctanoic acid (PFOA). *Toxicol. Sci.* **89,** 93–107.

Hamadeh, H. K., Bushel, P. R., Jayadev, S., Martin, K., DiSorbo, O., Sieber, S., Bennett, L., Tennant, R., Stoll, R., Barrett, J. C., *et al.* (2002). Gene expression analysis reveals chemical-specific profiles. *Toxicol. Sci.* **67,** 219–231.

Helma, C. (2005). In silico predictive toxicology: The state-of-the-art and strategies to predict human health effects. *Curr. Opin. Drug Discov. Dev.* **8,** 27–31.

Horie, M., Hayashi, M., Satoh, T., Hotta, H., Nagata, Y., Ishida, F., and Kamei, T. (1993). An inhibitor of squalene epoxidase, NB-598, suppresses the secretion of cholesterol and triacylglycerol and simultaneously reduces apolipoprotein B in HepG2 cells. *Biochim. Biophys. Acta* **1168,** 45–51.

Huber, W., von Heydebreck, A., Sultmann, H., Poustka, A., and Vingron, M. (2002). Variance stabilization applied to microarray data calibration and to the quantification of differential expression. *Bioinformatics* **18**(Suppl. 1), S96–S104.

Le Quere, V., Plee-Gautier, E., Potin, P., Madec, S., and Salaun, J. P. (2004). Human CYP4F3s are the main catalysts in the oxidation of fatty acid epoxides. *J. Lipid Res.* **45,** 1446–1458.

Letteron, P., Sutton, A., Mansouri, A., Fromenty, B., and Pessayre, D. (2003). Inhibition of microsomal triglyceride transfer protein: Another mechanism for drug-induced steatosis in mice. *Hepatology* **38,** 133–140.

Lumley, C. E., and Walker, S. R. (1987a). Predicting the safety of medicines from animal toxicity tests. I. Rodents alone. *Arch. Toxicol. Suppl.* **11,** 295–299.

Lumley, C. E., and Walker, S. R. (1987b). Predicting the safety of medicines from animal toxicity tests. II. Rodents and non-rodents. *Arch. Toxicol. Suppl.* **11,** 300–304.

Richards, V. E., Chau, B., White, M. R., and McQueen, C. A. (2004). Hepatic gene expression and lipid homeostasis in C57BL/6 mice exposed to hydrazine or acetylhydrazine. *Toxicol. Sci.* **82,** 318–332.

Ruan, H., and Pownall, H. J. (2001). Overexpression of 1-acyl-glycerol-3-phosphate acyltransferase-alpha enhances lipid storage in cellular models of adipose tissue and skeletal muscle. *Diabetes* **50,** 233–240.

Sanders, R. J., Ofman, R., Valianpour, F., Kemp, S., and Wanders, R. J. (2005). Evidence for two enzymatic pathways for omega-oxidation of docosanoic acid in rat liver microsomes. *J. Lipid Res.* **46,** 1001–1008.

Satoh, T., Hidaka, Y., and Kamei, T. (1990). Regulation of squalene epoxidase activity in rat liver. *J. Lipid Res.* **31,** 2095–2101.

Storck, T., von Brevern, M. C., Behrens, C. K., Scheel, J., and Bach, A. (2002). Transcriptomics in predictive toxicology. *Curr. Opin. Drug Discov. Dev.* **5,** 90–97.

Suter, L., Babiss, L. E., and Wheeldon, E. B. (2004). Toxicogenomics in predictive toxicology in drug development. *Chem. Biol.* **11,** 161–171.

Tachibana, K., Kobayashi, Y., Tanaka, T., Tagami, M., Sugiyama, A., Katayama, T., Ueda, C., Yamasaki, D., Ishimoto, K., Sumitomo, M., *et al.* (2005). Gene expression profiling of potential peroxisome proliferator-activated receptor (PPAR) target genes in human hepatoblastoma cell lines inducibly expressing different PPAR isoforms. *Nucl. Recept.* **3,** 3.

Troyanskaya, O., Cantor, M., Sherlock, G., Brown, P., Hastie, T., Tibshirani, R., Botstein, D., and Altman, R. B. (2001). Missing value estimation methods for DNA microarrays. *Bioinformatics* **17,** 520–525.

Waterham, H. R., Koster, J., Romeijn, G. J., Hennekam, R. C., Vreken, P., Andersson, H. C., FitzPatrick, D. R., Kelley, R. I., and Wanders, R. J. (2001). Mutations in the 3beta-hydroxysterol Delta24-reductase gene cause desmosterolosis, an autosomal recessive disorder of cholesterol biosynthesis. *Am. J. Hum. Genet.* **69,** 685–694.

Wechsler, A., Brafman, A., Shafir, M., Heverin, M., Gottlieb, H., Damari, G., Gozlan-Kelner, S., Spivak, I., Moshkin, O., Fridman, E., *et al.* (2003). Generation of viable cholesterol-free mice. *Science* **302,** 2087.

Westphal, J. F., Vetter, D., and Brogard, J. M. (1994). Hepatic side-effects of antibiotics. *J. Antimicrob. Chemother.* **33,** 387–401.

Wu, Z., Bucher, N. L., and Farmer, S. R. (1996). Induction of peroxisome proliferator-activated receptor gamma during the conversion of 3T3 fibroblasts into adipocytes is mediated by C/EBPbeta, C/EBPdelta, and glucocorticoids. *Mol. Cell Biol.* **16,** 4128–4136.